

# Alternative description of particle shower longitudinal profile

Samvel Ter-Antonyan\*

*Department of Physics, Southern University, Baton Rouge, Louisiana, 70813, USA*  
 (Received 17 March 2015; published 26 May 2015)

An alternative parametrization of the particle shower longitudinal profile is presented. The accuracy of the obtained shower profile description is about 2–3% for the 0 – 1500 g/cm<sup>2</sup> atmosphere slant depths and primary H, He, ...Fe nuclei in the 1 PeV–10 EeV energy range. It is shown that the shape of the shower profile depends only on the nucleon energy, whereas the maximum shower size also depends on the energy of the parental nucleus. Results are based on the CORSIKA simulated shower profiles and are presented in comparison with the Gaisser-Hillas parametrization.

DOI: [10.1103/PhysRevD.91.103005](https://doi.org/10.1103/PhysRevD.91.103005)

PACS numbers: 96.50.S-, 96.50.sd, 96.50.sb

## I. INTRODUCTION

The parametrization of longitudinal profiles for particle showers produced by primary nuclei in the atmosphere is an essential tool for the identification of primary nuclei and the evaluation of primary energy. Experiments that sample the shower longitudinal development using Cherenkov light images [1] or air fluorescence [2,3] from different traversed atmospheric depths extract the position of the shower maximum, which is sensitive to the incident primary nucleus. The integral of the shower profile is strongly correlated with the primary energy [4].

The shower longitudinal profile is a dependence of the shower particle number ( $N$ ) on a given traversed atmospheric depth,  $T$ . The parametrization of the shower profile commonly used in cosmic-ray experiments is the Gaisser-Hillas formula [5]:

$$N(X) = N_{\max} \left( \frac{X}{X_{\max}} \right)^{X_{\max}} \exp(X_{\max} - X), \quad (1)$$

where  $X = (T - X_0)/\lambda$  and  $X_{\max} = (T_{\max} - X_0)/\lambda$ .

The maximum number of shower particles  $N_{\max}$  at the traversed atmospheric depth  $T_{\max}$  along with  $X_0$  and  $\lambda$  in Eq. (1) are free parameters that depend on the primary nucleus and energy.

The standard primary nuclei composition consists of the first 28 nuclei of the periodic table with mass (nucleon) numbers  $A = 1, \dots, 56$ , usually divided into four to six groups (species): H, He, CNO-like, Si-like, and Fe-like. The large number of nuclei species (more than four) increases the uncertainties of the inverse problem ( $E$  and  $A$  reconstruction), falsely improving the agreement of experiment with theory [6].

The primary energy region responsible for particle shower detection at the observation level begins at about  $E > 1$  PeV and ends at Greisen-Zatsepin-Kuzmin cutoff energies [2].

The efficiency of the four-parameter parametrization (1) is in its applicability to a wide range of energies and primary nuclei. However, the observed correlations between parameters result in a loss of the physical meaning of  $X_0$  and  $\lambda$  [7] and reduce the range of effective atmospheric depths for Eq. (1).

## II. PARAMETRIZATION

Here, an alternative parametrization  $N(T, E, \epsilon)$  for the particle shower longitudinal profile is proposed using three noncorrelating parameters that depend on the primary particle energy and nucleon energy,  $\epsilon$ :

$$N(x) = N_{\max} \exp \left( -\frac{1}{2} \left( \frac{\ln x}{\delta(x)} \right)^2 \right), \quad (2)$$

where

$$\delta(x) = \alpha - \beta (\tanh x)^{\frac{1}{4}} \quad (3)$$

is the profile shape function of the variable

$$x = \frac{T}{T_{\max}}.$$

The shower maximum position,  $T_{\max}(\epsilon)$ , and shape function,  $\delta(x, \epsilon)$ , turn out to be dependent on the primary particle energy per nucleon,

$$\epsilon = \frac{E}{A}, \quad (\text{PeV/n}).$$

The maximum number of shower particles  $N_{\max}(E, \epsilon)$  is factored into the primary energy and a function of the nucleon energy only. The corresponding approximations for the parameters of the shower longitudinal profile (2)–(3) are

$$\alpha = 0.707 + 0.209\epsilon^{-0.084}, \quad \beta = \sqrt{\alpha/2.59}, \quad (4a)$$

\* samvel@icecube.wisc.edu

$$T_{\max} = 433.5 + 38.9(\ln(\epsilon A_{\text{Fe}}))^{0.857}, \quad (\text{g/cm}^2), \quad (4b)$$

$$N_{\max} = 0.653(E/1 \text{ GeV})(1 - e^{-2.5\epsilon^{0.12}}), \quad (4c)$$

where  $A_{\text{Fe}} = 56$  and  $\epsilon$  is in the units of PeV/n. The goodness-of-fit tests for Eqs. (4a)–(4c) give  $\chi^2 < 1$  at negligible correlations between the  $\alpha$ ,  $T_{\max}$ , and  $N_{\max}$  parameters.

### III. SHOWER PROFILES

The values of the free parameters in Eqs. (1) and (2) were obtained from simulated shower profiles (training sample) using the CORSIKA [8] (SIBYLL [9]) code for four primary nuclei  $A \equiv 1, 4, 16, 56$  at six energies  $E \equiv 1, 10, 100, 500, 2500, 10^4$  PeV. Shower profiles were studied for ten atmospheric depths  $T \equiv 100, 200, \dots, 1000 \text{ g/cm}^2$  at two zenith angles,  $\cos\theta = 0.7$  and 1. The shower particle energy threshold was  $E_e > 1 \text{ MeV}$ . Simulation statistics were provided for less than 2–3% statistical errors in the whole measurement range.

The averaged shower profiles were approximated by Eqs. (1) and (2) using 13 reference depths. The results are presented in Fig. 1. It is seen that the parametrization (1) (dashed lines) underestimates the shower sizes at large atmospheric depths.

The parametrization errors of Eqs. (1) and (2) and the corresponding  $\chi^2_{\text{d.o.f}}$  are presented in Fig. 2 for different primary energies and nuclei. The upper and middle panels show the errors of the four-parameter approximations of

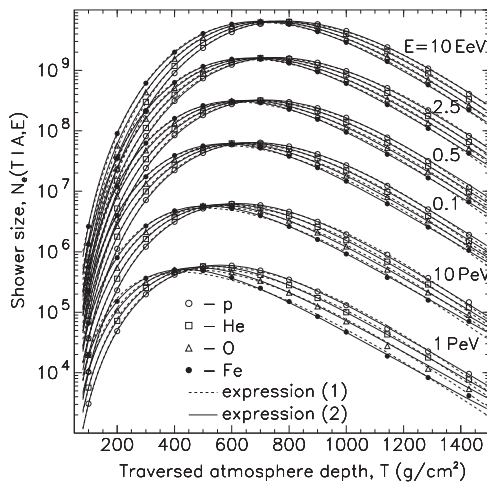


FIG. 1. Average longitudinal shower profiles for 13 traversed atmospheric depths produced by H, He, O, and Fe primary nuclei with six energies (from 1 PeV to 10 EeV). The symbols are CORSIKA shower simulated data (training sample). The dashed lines are results from the four-parameter approximation (1). The solid lines are the parametrizations (2)–(4) computed for corresponding primary nuclei and energies.

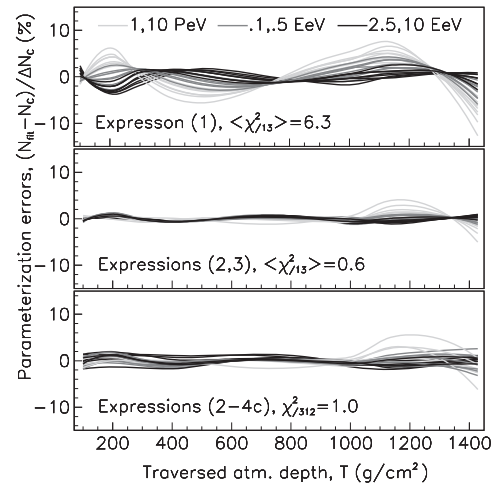


FIG. 2. Parametrization errors  $(N_{\text{fit}} - N_{\text{corsika}}) / \Delta N_{\text{corsika}}$  for the four-parameter expressions (1) and (2)–(3) are shown in the upper and middle panels, respectively. The lower panel corresponds to the errors of the shower profiles  $N(T, A, E)$  from Eqs. (2)–(4) for different primary energies and nuclei.

CORSIKA simulated shower profiles using the  $N_{\max}$ ,  $T_{\max}$ ,  $X_0$ , and  $\lambda$  parameters of Eq. (1) and the  $N_{\max}$ ,  $T_{\max}$ ,  $\alpha$ , and  $\beta$  of Eqs. (2) and (3). The lower panel of Fig. 2 shows the errors of the shower profiles  $N(T, E, A)$  from Eqs. (2)–(4).

The normalized simulated (symbols) and parametrized (lines) shower profiles are presented in Fig. 3. It is seen that parametrization (2) effectively describes the shower profiles in the regions of both the maximum ( $x \approx 1$ , inset figure, solid line) and asymptotic depths ( $x \approx 3$ ). Equation (1) is systematically biased by about  $-2\%$  (inset figure, dashed line) at  $x \approx 1$ .

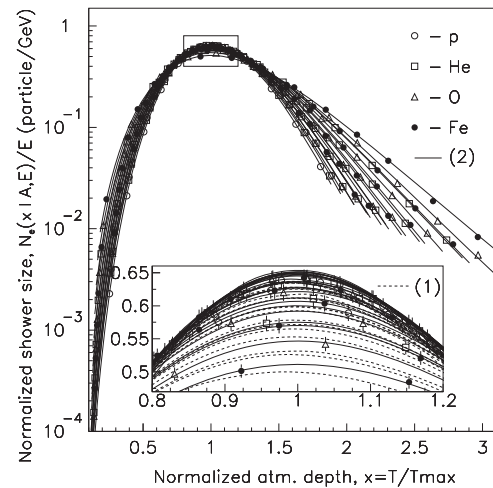


FIG. 3. Normalized particle shower profiles. The symbols are CORSIKA simulated data (training sample). The lines are the results of the parametrization (2). The inset figure is a zoom of the selected rectangular region for  $0.8 < x < 1.2$ . The dashed lines correspond to the parametrization (1).

#### IV. PARAMETERS

The studies of the dependence of  $T_{\max}(\epsilon)$  and  $N_{\max}(\epsilon)$  on the nucleon energy ( $\epsilon$ ) are presented in the upper and lower panels of Fig. 4, respectively. The approximations of shower profiles using parametrizations (1) and (2) were trailed for different lower ( $T_{\text{low}}$ ) and upper ( $T_{\text{up}}$ ) limits of traversed atmospheric depth.

The estimated values for  $T_{\max}$  (Fig. 4, upper panel) were unbiased for all trails. The line in Fig. 4 corresponds to Eq. (4b). The asterisk and cross symbols in Fig. 4 are correspondingly renormalized CORSIKA simulated data from Ref. [10].

Estimations of  $N_{\max}$  (Fig. 4, lower panel) using Eq. (1) for approximations of the shower profile turned out to be dependent on boundary conditions for the atmospheric depth (hollow and bold star symbols), whereas Eq. (2) remained practically unbiased (hollow and bold circle symbols) for different boundaries.

The shower profile shape functions  $\delta(\epsilon|T)$  and  $\delta(x|\epsilon)$  are presented in Fig. 5, where the symbols (left panel) are the data extracted from the CORSIKA simulated training sample. The solid lines in both panels correspond to Eqs. (3) and (4a). The dashed lines in the right panel of Fig. 5 are the 0.5% accuracy logarithmic simplifications of the shape function (3),

$$\delta(x) \cong \begin{cases} a - b \ln x, & \text{if } 0.07 \lesssim x \leq 1, \\ a - b \ln x / (1 + 1.59 \ln x), & \text{if } x > 1, \end{cases} \quad (5)$$

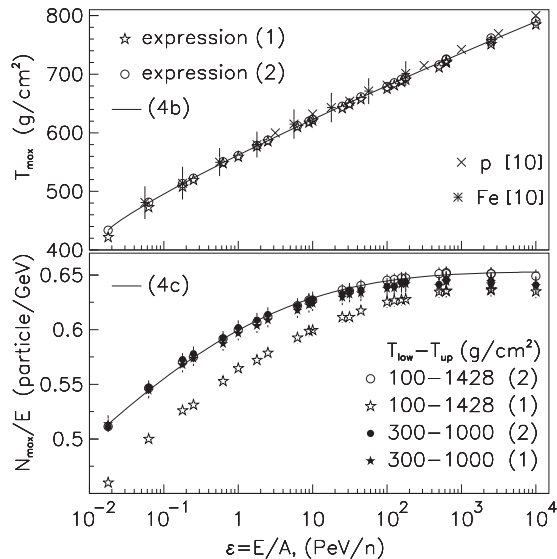


FIG. 4. Parameters  $T_{\max}$  (upper panel) and  $N_{\max}/E$  in units of particle/GeV (lower panel) derived from Eqs. (1) and (2) for the different boundaries of traversed depths. The lines correspond to Eqs. (4b) and (4c) for  $T_{\max}$  and  $N_{\max}$ , respectively.

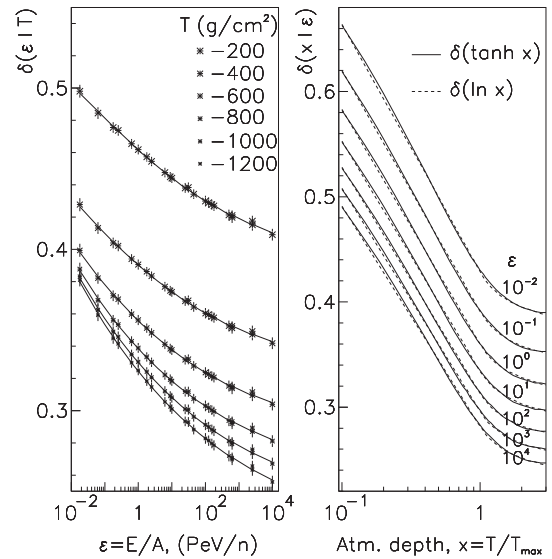


FIG. 5. Shower profile shape function [Eq. (3)] depending on the nucleon energy (left panel) and normalized atmospheric depth (right panel). The solid lines correspond to Eqs. (3) and (4a). The dashed lines in the right panel are the logarithmic simplifications of the shape function according to Eqs. (5) and (6).

where

$$a = 0.215 + 0.145\epsilon^{-0.084}, \quad b = 0.086 + 0.011\epsilon^{-0.084}, \quad (6)$$

at  $\chi^2/450 = 0.7$ . The approximation (5) provides the analytic solutions of the inverse functions  $N_0^{-1}(x)$  for  $x < 1$  and  $N_1^{-1}(x)$  for  $x > 1$ .

#### V. VERIFICATION

The verification of the universality of approximations (1) and (2) was performed by extrapolating the shower profiles from the 100 – 1428 g/cm<sup>2</sup> interval to the  $T = 10$  g/cm<sup>2</sup> observation level, corresponding to the earlier stage of shower development. The results are presented in Fig. 6. The symbols at  $T = 10$  g/cm<sup>2</sup> in Fig. 6 are the corresponding data from the CORSIKA simulated control sample, whereas the symbols at  $T = 100$  g/cm<sup>2</sup> are the representatives of the training sample (Sec. III).

It is seen that the parametrization (1) (being trained in the 100 – 1428 g/cm<sup>2</sup> depth interval) cannot be extrapolated to the region less than about 50 g/cm<sup>2</sup> (lines, left panel), whereas the parametrization (2) works correctly up to the beginning of the atmosphere (lines, right panel).

The verifications of the shower profiles (2)–(4) by the control samples of different nuclei and energies are shown in Fig. 7. The shower profile for a primary Fe nucleus with energy  $E = 500$  PeV and corresponding  $\epsilon \approx 8.93$  PeV/n from the training sample (Sec. III) are compared to the

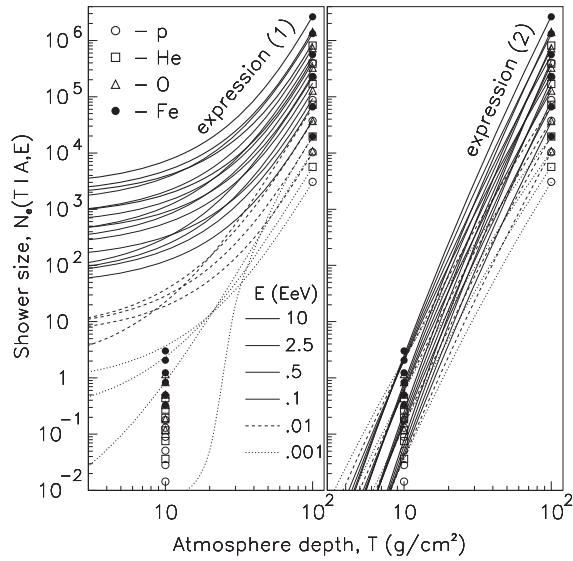


FIG. 6. Extrapolations of the parametrizations (1) (left panel) and (2) (right panel) to the earliest stage of shower development for different primary nuclei and energies (lines). Symbols are the CORSIKA simulated data.

control sample of shower profiles produced by primary H, He, C, O, and Si nuclei with the same energy per nucleon (symbols). The lines in Fig. 7 are the corresponding congruent predictions from the parametrizations (2)–(4).

The results in Fig. 7 confirm the  $\epsilon$  dependence of the shower longitudinal profile shape [Eqs. (4a) and (4b)]. The shower profile amplitude ( $N_{\max}$ ) also depends linearly on the primary energy,  $E$  [Eq. (4c)].

The good agreement in Fig. 7 between predictions (lines) and simulated data indicates the correctness of Eqs. (2)–(4)

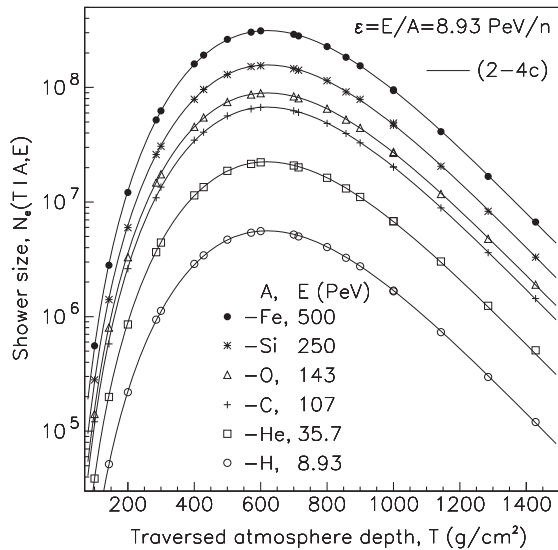


FIG. 7. Control samples of shower profiles (symbols) produced by the different primary nuclei with the same nucleon energy  $\epsilon \approx 8.93$  PeV/n. The lines are the predictions from Eqs. (2)–(4).

for the shower profile description at least with accuracies of about 2–3% in the whole measurement range.

## VI. INTEGRAL

The right-hand side of Eq. (2) at the corresponding normalization can be considered as a probability density function and can be used for primary energy evaluation [2,4]. Unfortunately, this function was missed by mathematicians, and by using a numerical technique the required normalization

$$\int_0^\infty f(x, \epsilon) dx \approx 1 \pm 10^{-4} \quad (7)$$

was provided for the probability density function

$$f(x) = \frac{1}{\sqrt{2\pi}\delta_0} \exp\left(-\frac{1}{2}\left(\frac{\ln x}{\delta(x)}\right)^2\right) \quad (8)$$

with the additional parameter

$$\delta_0 = 0.226 + 0.148\epsilon^{-0.092}.$$

The goodness-of-fit test for  $\delta_0(\epsilon)$  was  $\chi^2 = 0.01$  in the  $10^{-2} \leq \epsilon \leq 10^4$  (PeV/nucleon) interval and the upper limit of the integral (7),  $x_{\max} = 3$ .

It is interesting to note the relation between the parameters  $\delta_0$  and shape function  $\delta(x)$  from Eq. (3):

$$\delta_0(\epsilon) \approx \frac{1}{x_{\max}} \int_0^{x_{\max}} \delta(x) dx \pm 1\%. \quad (9)$$

The statistical parameters—the average ( $\bar{x}$ ) and standard deviation ( $\sigma_x$ ) of the distribution (8)—are well approximated (0.1% errors) by the following expressions that depend on the nucleon energy:

$$\bar{x} = 1.036 + 0.094\epsilon^{-0.12}$$

at  $\chi^2 = 0.1$ , and

$$\sigma_x = 0.226 + 0.176\epsilon^{-0.092}$$

at  $\chi^2 = 1.1$ .

## VII. FLUCTUATIONS

The main source of shower profile fluctuations is the depth of the first interaction of primary particles in the atmosphere [11]. The exponentially distributed uncertainty of the first interaction point results in the corresponding fluctuations of the shower profile (2) depending on the rate of change ( $dN/dx$ ) of the profile with respect to the depth,  $x$ . Thus, the fluctuations should be maximal at the beginning of shower development ( $x \approx 0$ , Fig. 3), and minimal in the region of shower maximum,  $x = 1$ . The dependence of the interaction length,  $\lambda(A, E)$ , on the primary particle also

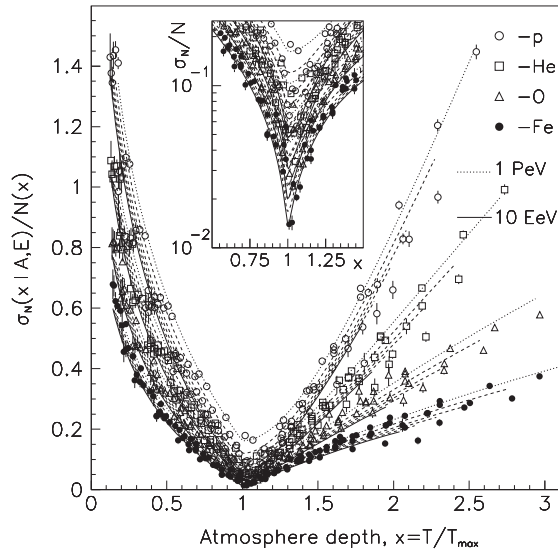


FIG. 8. Normalized standard deviations ( $\sigma_N/N$ ) of shower particles for different primary nuclei and primary energies (symbols). The lines represent the parametrization (10) for energies of 1 PeV (dotted lines) and 10 EeV (solid lines). The dashed lines describe the fluctuations for intermediate energies. The inset panel zooms in on the region of minimal fluctuations at  $x \approx 1$ .

results in the mass ( $A$ ) and energy ( $E$ ) dependencies of the shower profile fluctuations.

The statistical measure of fluctuations is the standard deviation of the shower particle number,  $\sigma_N$ . The corresponding values of  $\sigma_N(x, A, E)/N(x)$  obtained from the shower simulated data set (Sec. III) are presented in Fig. 8 (symbols). The inset panel shows the region of minimal fluctuations in detail. The lines in Fig. 8 correspond to the parametrizations

$$\frac{\sigma_N}{N} \approx \begin{cases} a_1 - a_2 \ln x, & \text{if } x \leq 1, \\ a_1 + a_3 (\ln^{\eta} x)/x, & \text{if } x > 1, \end{cases} \quad (10)$$

where

$$\begin{aligned} a_1 &= 0.165A^{-0.32}E^{-0.13}, \\ a_2 &= 0.68A^{-0.185}E^{-0.009}, \\ a_3 &= 3.77A^{-0.386}E^{-0.035}, \\ \eta &= 2.67A^{-0.080}E^{-0.027} \end{aligned}$$

at  $\chi^2/470 \approx 1.7$ .

## VIII. SUMMARY

The standard inverse problem of cosmic-ray physics in the PeV–EeV energy region is the identification of a

primary nucleus (or elemental composition) and the estimation of its energy (or energy spectrum) by the detected shower response at the observation level in the frames of a given interaction model. The efficiencies of the primary particle and primary energy estimators depend on both the accuracy (Sec. III) and universality (Sec. V) of the shower longitudinal profile description.

Historically, the conventional shower longitudinal profiles were proposed in 1960 (Greisen function) [12], 1977 (Gaisser-Hillas function) [5], and 2001 (Gaussian-In-Age approach) [13]. The efficiencies and accuracies of the listed profile parametrizations were compared in Refs. [4,14,15] in detail.

The last Gaussian-In-Age approach [4] reduced the number of parameters to three, and decreased the inter-correlations between the parameters of the profile function in return for the narrow range of applicability in the vicinity of shower maximum:  $0.75 \lesssim s \lesssim 1.25$  [14], where  $s = 3/(1 + 2/x)$  is the shower age parameter.

The alternative shower longitudinal profile description [Eqs. (2)–(4)], as opposed to the parametrizations [4,5,12], represents the first complete formula for the shower profile,  $N(T, A, E)$ , depending on atmospheric depth ( $T$ ), the primary nucleus ( $A$ ), and primary energy  $E$ . Equations (2)–(4) provide accuracies of about 2–3% for the region  $0 < T \leq 1450 \text{ g/cm}^2$ ,  $A \leq 56$ ,  $1 \text{ PeV} \leq E \leq 10 \text{ EeV}$ . The results were obtained in the frames of the SIBYLL [9] interaction model (Sec. III).

The position of the shower maximum  $T_{\max}(\epsilon)$  from Eq. (4b) and the profile shape function  $\delta(x, \epsilon)$  from Eq. (4a) depend only on the primary nucleon energy  $\epsilon = E/A$ , which is in agreement with the prediction of the superposition model [16].

The amplitude of the profile  $N_{\max}(E, \epsilon)$  from Eq. (4c) depends on both the primary energy ( $E$ ) and nucleon energy ( $\epsilon$ ).

The intercorrelations between the  $N_{\max}(E, \epsilon)$ ,  $T_{\max}(\epsilon)$ , and  $\delta(x, \epsilon)$  shower profile parameters are negligible.

The profile shape function,  $\delta(x, \epsilon)$ , from Eq. (3) has the simple logarithmic representation (5), which provides an analytic solution for the corresponding inverse profile function, which can be used in the constant-intensity-cut method [5].

The fluctuations of the particle shower longitudinal profile,  $\sigma_N/N$ , from the parametrization (10) depend on the energy ( $E$ ) and mass number ( $A$ ) of the primary nuclei.

## ACKNOWLEDGMENTS

I wish to thank James Matthews for useful correspondence.

- [1] T. Abu Zayyad *et al.* (HiRes-MIA Collaboration), *Astrophys. J.* **557**, 686 (2001).
- [2] J. Abraham *et al.* (Auger Collaboration), *Phys. Lett. B* **685**, 239 (2010).
- [3] H. Tokuno *et al.* (Telescope Array Collaboration), *Nucl. Instrum. Methods Phys. Res., Sect. A* **676**, 54 (2012).
- [4] J. A. J. Matthews, R. Mesler, B. R. Becker, M. S. Gold, and J. D. Hague, *J. Phys. G* **37**, 025202 (2010).
- [5] T. K. Gaisser and A. M. Hillas, in *Proceedings of the 15th International Cosmic Ray Conference, Bulgarian Academy of Sciences, Plovdiv, Bulgaria, August 13–26, 1977* (Bulgarian Academy of Sciences, Sofia, 1977), p. 353.
- [6] S. Ter-Antonyan, *Phys. Rev. D* **89**, 123003 (2014).
- [7] J. M. C. Montanus, *Astropart. Phys.* **35**, 651 (2012).
- [8] D. Heck *et al.*, Report No. FZKA 6019 (1998).
- [9] R. S. Fletcher, T. K. Gaisser, P. Lipari, and T. Stanev, *Phys. Rev. D* **50**, 5710 (1994).
- [10] S. P. Swordy *et al.*, *Astropart. Phys.* **18**, 129 (2002).
- [11] T. Stanev, *High Energy Cosmic Rays* (Springer, New York, 2010).
- [12] K. Greisen, *Annu. Rev. Nucl. Sci.* **10**, 63 (1960).
- [13] T. Abu-Zayyad *et al.* (HiRes Collaboration), *Astropart. Phys.* **16**, 1 (2001).
- [14] C. Song, *Astropart. Phys.* **22**, 151 (2004).
- [15] A. Aab *et al.* (Pierre Auger Collaboration), *Phys. Rev. D* **90**, 122005 (2014).
- [16] P. Sommers, *C.R. Phys.* **5**, 463 (2004).